DOI: 10.1002/cbic.200700313

Analysis of Organo–Silica Interactions during Valve Formation in Synchronously Growing Cells of the Diatom *Navicula pelliculosa*

Alejandro Heredia,*[a] Han J. van der Strate,[b] Ivonne Delgadillo,[c] Vladimir A. Basiuk,[a] and Engel G. Vrieling[d]

Biologically formed silica is produced at ambient conditions under the control of molecular and physicochemical processes that are apparently integrated in biosilica morphogenesis, but the mechanisms are not yet fully understood. With the recent identification of small polypeptides and proteins that are encapsulated inside the biosilica and functional in silica polymerization in vitro, it is of importance to determine whether interactions between inorganic silica species and these organic compounds occur in vivo. A time-resolved analysis of valve formation in synchronously growing cells of the diatom species Navicula pelliculosa *enabled us to characterize the relevant chemical bonds by attenuated total reflectance Fourier-transformed infrared (ATR-FTIR) spectroscopy. Typically, inorganic bonds of Si–O–Si (bands at 1058, 843 cm^{-1}), Si–OH (3689 cm^{-1}), and P=O (1239 cm^{-1}) and organic bonds of proteinaceous matter (with the amide I and II bands at 1642 and 1543 cm^{-1}, respectively) were positively identified during one cycle of valve formation. The observed variations in FTIR band intensity and location represented specific interactions between organic and inorganic molecules during the major silicification event, during which stretching of the Si–O bonds was predominantly noticed. The experimentally obtained frequencies (ν) of the major bonds corresponded to those that were obtained by MM+ and PM3 FTIR simulations for organo–silica interactions based on biomolecules that are proposed to be involved in biosilica formation. The results indicated that hydrogen bonds originated from interactions, albeit weak, between organic phosphate or amine groups to the inorganic hydroxyl groups or oxygen atoms from the silicic acid and/or silica. The existence of covalent P–O–Si bonds and electrostatic interactions could not be excluded. These interactions clearly suggest that biomolecules actively contribute to the silica polymerization process during valve formation in* N. pelliculosa*, and also might act comparably in other diatoms species in which similar biomolecules have been identified.*

Introduction

The most distinctive silica producers in aquatic ecosystems are the unicellular algae known as diatoms, of which well over 10000 distinct species are taxonomically classified based on their intriguing siliceous exoskeleton morphology.[1] As is well known, the diatom cell walls are made of nanostructured amorphous silica (SiO_2) with a hierarchically ordered porous structural design[2,3] that exceeds current nanotechnological manufacturing capabilities.[4] Similar to other biominerals, biologically formed silica (or biosilica) is produced by controlled mechanisms under ambient conditions. Moreover, the molecular and physicochemical mechanisms in biosilica morphogenesis appear to be integrated; their combinatorial roles, however, are not yet well understood.[5,6] Diatoms prefer silicic acid [$Si(OH)_4^-$] monomers as a source of silicon, which then is processed by depositioning of the species-specific siliceous structures.

Recent studies on the formation of biosilica have focused on the evolution of colloidal chemistry in silicifying organisms, the molecular and physicochemical mechanisms of silicon biomineralization, and biomimetics of the ambient silicification processes for innovative silica-based materials in nanoscience and the silica industry.[4,7–9] In understanding biosilica formation, it is important to know whether and how organic and inorganic components interact in vivo. Such interactions can be expected to occur at two different organizational levels, 1) the interaction between the inorganic silicic acid ions and small biomolecules during silica precipitation, and 2) the interaction

[a] Dr. A. Heredia, Dr. V. A. Basiuk
Departamento de Química de Radiaciones y Radioquímica
Instituto de Ciencias Nucleares
Universidad Nacional Autónoma de México
Circuito Exterior C.U. Apdo. Postal 70-543
04510 México, D.F. (México)
Fax: (+52) 55-56-16-22-33
E-mail: aheredia@nucleares.unam.mx

[b] Dr. H. J. van der Strate
Department of Ocean Ecosystems
Centre for Ecological and Evolutionary Studies
University of Groningen
P.O. Box 14, 9750AA Haren (The Netherlands)

[c] Dr. I. Delgadillo
Unidade de Química Orgânica
Produtos Naturais e Agroalimentares, Department of Chemistry
Campus Universitário de Santiago, University of Aveiro
3810-193 Aveiro (Portugal)

[d] Dr. E. G. Vrieling
Groningen Biomolecular Sciences and Biotechnology Institute
University of Groningen
P.O. Box 14, 9750AA Haren (The Netherlands)

Supporting information for this article is available on the WWW under http://www.chembiochem.org or from the author.

 © 2008 Wiley-VCH Verlag GmbH & Co. KGaA, Weinheim

between larger biopolymers and oligomeric silica species and/or solid silica in morphogenesis. The occurrence of the first has been proposed from in vitro studies to determine the role of isolated peptides and polyamines from diatoms in silica precipitation.[11,21] The suggested phase-separation processes also indicate that these interactions might continue at a higher organizational levels.[10,11] Throughout the latter process, silicic acid and/or silica interactions with lipids and carbohydrates that are part of the membrane of the silica deposition vesicles (SDV) and subsequently the protective casing, seems also obvious.[12] Therefore, unraveling the processes that are involved in silicic acid polycondensation in vivo will lead to a further understanding of the mechanisms of biological nanopatterning, and how molecular and physicochemical aspects contribute.

Nevertheless, the occurrence of these interactions has not been demonstrated accurately. On the one side, non-invasive in vivo approaches are not readily available, whereas on the other side, the exact nature and composition of inorganic and organic molecules that induce or remain present during and after silica depositioning are not known. With respect to the latter, however, progress has been made for diatom and sponge biosilicas, and the biomolecular content such as silicon transporters, casing proteins, small encapsulated polypeptides (silaffins, silicatein), and long-chain polyamines (LCPAs) have been identified and characterized.[8,13–18] Also, the physicochemical properties of the diatom biosilica, particularly the specific surface area, fractality, surface roughness, and pore volumes and distributions have been well documented.[3,6,19,20]

In the pennate diatom *Navicula salinarum*, it has been demonstrated that valve morphogenesis is a rapid process with distinct stages in two- and three-dimensional valve development.[21] Apparently, diatom biosilica formation is a highly dynamic process, during which interactions between silicic acid and/or oligomeric silica species with organic molecules expectedly are of importance for growth and structure direction. Silica–biomolecule interactions in organisms have been studied in only a few instances, namely during silica formation that is induced by the exterior surface of bacteria,[22,23] and in the functioning of a cell-wall-associated diatomaceous carbonic anhydrase.[24,25] A time-resolved analysis of the evolution of chemical bonds due to interactions of inorganic and organic molecules in the course of diatom valve formation has not been encountered. Such a study could further substantiate the role of these interactions in silica depositioning, and perhaps elucidate structure–direction processes in diatom biosilicification. Insight into these silica–biomolecule interactions is also of interest to tailor the (bio)physicochemical properties of a synthetic route for the production of highly hierarchically ordered silica structures, or to translate this knowledge to the design of novel high-performance silica-based materials.[4]

We approached this challenge by analyzing the different stages of valve formation in synchronously growing cells of the pennate diatom species *Navicula pelliculosa*. For this species, data on various organic and inorganic components and physicochemical properties are known. The biosilica of these species exhibit a low (specific) surface area, which is common for diatomaceous silica,[5,26] and indicates that this silica is condensed, or less hydrated compared to artificial silicas.[27] Diatom biosilica of the frustules is located at the exterior of the plasma membrane of the cells, and as such, is protected against spontaneous dissolution in their aquatic ecosystems by a quite inert organic casing. This casing covers the siliceous frustule elements such as valves and girdle bands.[28] The thickness of the casing and the casing/silica ratio can negatively affect FTIR analyses, and this has been demonstrated for the species *N. minima*, which has a casing of about 100 nm thickness.[19] In the present study we have performed an attenuated total reflectance FTIR spectroscopy on biosilica that was obtained from a related but much smaller species, *N. pelliculosa*, for which the organic layer is thin;[29] this ensures that the FTIR spectra were not obscured by the bonds of the casing components. For the interpretation of experimental data, interactions were also analyzed by so-called PM3 FTIR spectroscopy simulations based on the physicochemical properties of a few biomolecules that are known to be involved in biosilica formation, namely: native silaffins, LCPAs, and silicatein. Silaffins and LCPAs (or combinations thereof) exhibit the ability to induce silica precipitation in vitro, and, depending of the reaction conditions, control the morphology of the finally formed silicas; this has been extensively reviewed by Lopez et al.[8] and Foo et al.[14]

Results and Discussion

Valve formation in *N. pelliculosa*

Molecular probing of valve formation in *N. pelliculosa* by using 2-(4-pyridyl)-5-((4-(2-dimethylaminoethylamino-carbamoyl)methoxy)phenyl) oxazole (PDMPO) revealed that the new hypovalve was rapidly produced (Figure 1) and that the whole process proceeds comparably to the sequence that was observed for a closely related species, *N. salinarum*.[51] The premature valve appeared to originate from the center of the cells, starting at the central nodule in proximity to the cleavage furrow (arrow Figure 1 D). Already after 20 min, the newly formed valves were clearly recognized at the axial area (Figure 1 E and F) and continued to expand in the next 40 min towards the outer valve edges (Figure 1 G–J).

Development of the valve in the third dimension or valve thickening was readily observed at later intervals ($\geq$60 min; Figure 1 I–L), during which also the transapical costae could be identified, especially when the focal plane was adjusted manually (not shown here). From these observations, it was clear that silicification occurs mainly within the first hour (Figure 1 A–J), during which macromorphogenesis, that is the formation of the larger frameworks,[30] and micromorphogenesis, that is, the subsequent formation of detailed structures during valve thickening[30] were defined as distinct events. After 8 hours (Figure 1 K and L), cell separation has been initiated; this indicates completion of the new hypovalves; the cleavage furrow is well visible upon separation of the PDMPO-probed hypovalves (arrow in Figure 1 L).

 © 2008 Wiley-VCH Verlag GmbH & Co. KGaA, Weinheim

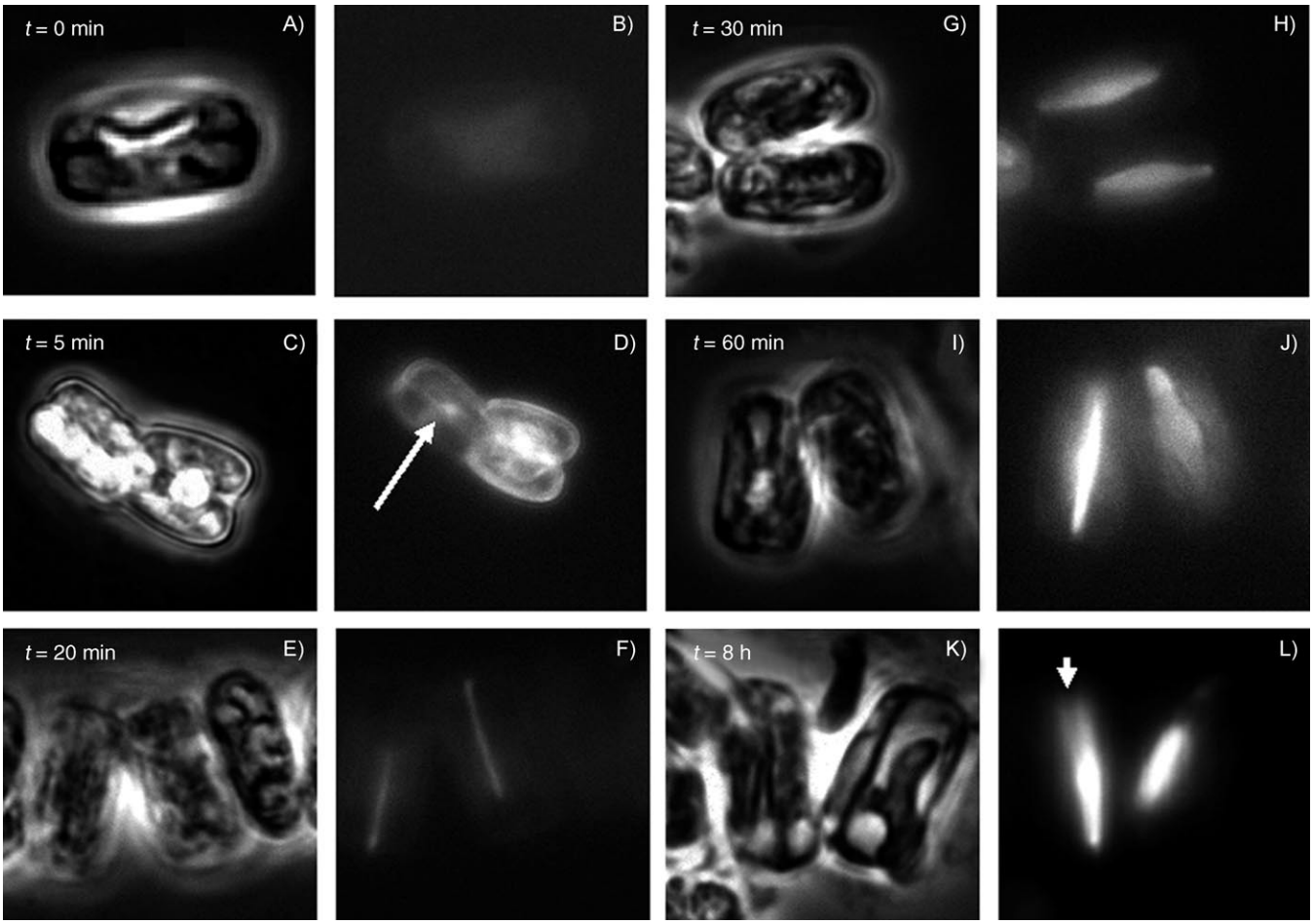

Figure 1. Valve formation in synchronously growing *Navicula pelliculosa* cells visualized by PDMPO probing. All images were taken from cells that were oriented in the girdle view. The fluorescence images (right columns) were aligned by their bright field ones (left columns). The sequence of valve formation is shown as the duration of valve formation after replenishment of silicon to Si-synchronized cells (see also Table 1 in the sampled intervals); note that $t=0$ (a,b) refers to the cells in cytokinetic arrest just prior to addition of silicic acid and PDMPO.

FTIR analysis on *N. pelliculosa* samples

The FTIR spectra were obtained for synchronously growing *N. pelliculosa* cells by subsampling over 1 cycle of valve formation. The collected subsamples represent snap-shots for a time-resolved analysis, for which harvested cells were studied as following: whole cells (Figure 2), analysis of the ratio between the initial stage and later stages (t_n/t_0; Figure 3), SDS-treated cells (Figure 4) and HNO_3-treated cells (Figure 5) that correspond to a diminished contribution of organic matter. All positively identified peaks that were used to assign bonds by the frequency (ν) are summarized per studied interval and treatment (Table 1). The spectra obtained from samples of whole cells displayed the most important fingerprints of silica as part of diatom frustules (Figure 2 A and B). The bands at ~1060 and 843 cm^{-1} were assigned as stretching vibrations of Si–O groups, and were clearly identified over all of the valve formation intervals. For whole cells however, a quite broad band at about 1058 cm^{-1} was noticed, which possibly originated from PO_4^{3-} from the organic molecules.[31] Other fingerprint bands that were present at all intervals were those of amide I at ~1642 cm^{-1} and amide II at ~1543 cm^{-1} (Figure 2); these bands refer specifically to the presence of proteins.[32] The broad band between 1000 and 1250 cm^{-1} with a maximum at ~1080 cm^{-1} (Figure 2 A and B) was identified as the most important band for inorganic matter because it represents the sum of many bonds and/or interactions that are related to silicon and phosphate groups (Figure 2 C).

This broad band most probably also includes the band of Si–O–C bonds at ~1080 cm^{-1} [34] and P–O–C bonds with bands at both ~1076 and 1085 cm^{-1}.[34] The occurrence of bands for the Si–C and P–O–Si groups (782–794 cm^{-1}) were not identified and their presence was ruled out.[35,36] Also covalent inorganic bonds between Si atoms and N or C atoms were not identified, this is in agreement with earlier observations.[37] Surprisingly, in the spectra of whole cells, two distinct bands were observed in parallel at different stages of valve formation; namely at the intervals of $t=30$, 50, 350 and 1440 min. The bands appeared at 1734 and 3689 cm^{-1} (Figure 2 B) and are respectively related to bonds of a C=O ester[19] and a C–OH or an O–H.[38,39] Our FTIR analysis did not provide information on the presence of other solids or mineral groups, such as sulfate.[40]

 © 2008 Wiley-VCH Verlag GmbH & Co. KGaA, Weinheim

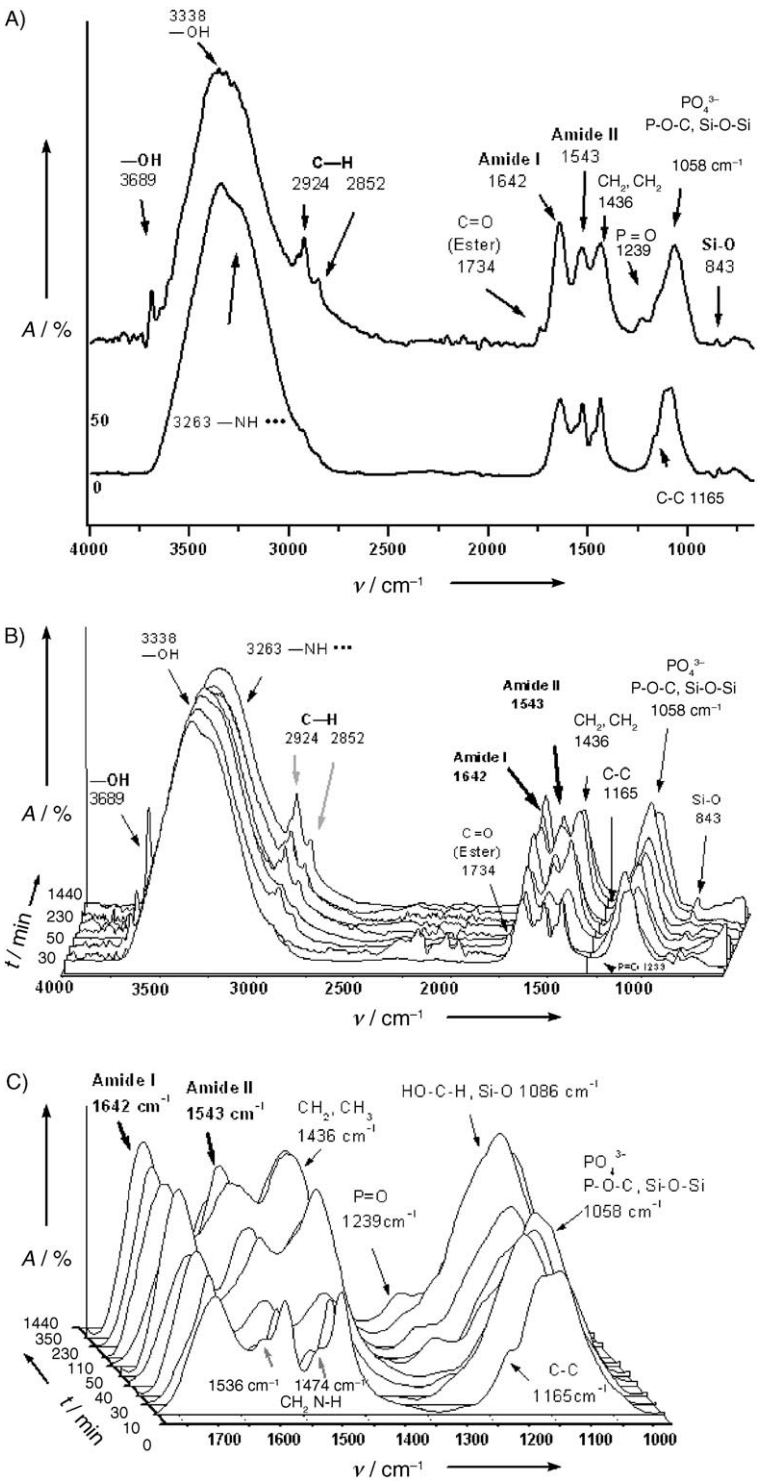

Figure 2. FTIR spectra of the whole cells of the diatom *Navicula pelliculosa*, which were collected during valve formation of synchronously growing cells (see also Table 1 for the sampling scheme). The most clear-cut peaks are indicated and assigned to previously reported bonds (see also Table 1). A) Two representative FTIR spectra at the starting stage ($t=0$; lower spectrum) and after 50 min of valve formation (upper spectrum) and B) normalized spectra that were obtained throughout the whole process of valve synthesis that indicate variations between bonds at different stages of valve formation. C) Normalized FTIR spectra for the region of 1770–950 cm^{-1}.

It should be noted that the band at 3689 cm^{-1} can also represent O–H stretching from highly ordered structures in relation to the chemical composition of the inorganic surface.[38] In diatomaceous silica, OH groups indeed are located at the silica surface.[5,41] The bands at 2924 and 2852 cm^{-1} (gray arrows Figure 2B) were assigned as C–H bonds (Table 1), which in general correspond to presence of hydrocarbons or lipids;[42–44] these bands, however, were not always clearly detectable during valve formation in these whole-cell samples.

Because of the importance of the 1770–950 cm^{-1} region, which concerns bonds between silicon and other atoms, the spectra have been normalized in order to determine whether the peak intensity and bond occurrence varied during the course of valve formation (Figure 2C). Indeed variations in peak location and intensity were observed; this suggests dynamics in the contribution of bonds and the content and composition of organic and inorganic matter in *N. pelliculosa* cells when new valves are produced. In the first stages of valve formation (between 0 and 10 min) two bands appeared in the region of 1563 and 1474 cm^{-1} (gray arrow Figure 2C) that most probably relate to the hydrogen-bond interaction between the amine group of a biomolecule and an oxygen from another molecule.[45] After 40 min of valve formation, an increase in the intensities of the amide I (1642 cm^{-1}) and amide II (1543 cm^{-1}) bands was observed (Figure 2C); this indicates that from this stage, protein synthesis co-occurred in synchronously growing *N. pelliculosa* cells. The presence of weak C–NH bonds (1563 and 1474 cm^{-1}; gray arrows Figure 2C) suggested that the deformation (stretching) of amine groups towards oxygen atoms of, for instance, silicic acid and/or silica, might have occurred. The bands near 1086 and 1058 cm^{-1} (Figure 2C), which coincided with Si–O and Si–O–Si bonds, seemed to change intermittently during valve formation. Especially, the Si–O–Si band at 1058 cm^{-1} coappeared with the P=O band at 1239 cm^{-1}, and this suggests that a biomolecule might have mediated the silicification process. The presence of the C–N–H stretching bands at 3263, 1563, and 1474 cm^{-1} (Figure 2A and C) in the earliest stage of valve formation (between 0 and 10 min) suggest an active interaction of biomolecules with inorganic compounds, most probably silicic acid and/or silica oligomers, in the first steps of silica polymerization.

For a qualitative analysis between the sampled intervals of valve formation in *N. pelliculosa*, an additional normalization step was applied that was based on a ratio analysis between every interval and the initial stage of cytokinesis arrest (t_0; Figure 3). In this way the obtained spectra at every later stage (t_n) was corrected for the contribution of the initial stage (t_0) and the relative difference between t_n and t_0 was determined; moreover, the ratio analysis enhanced the variations in the bond contributions between the compared stages,

 © 2008 Wiley-VCH Verlag GmbH & Co. KGaA, Weinheim

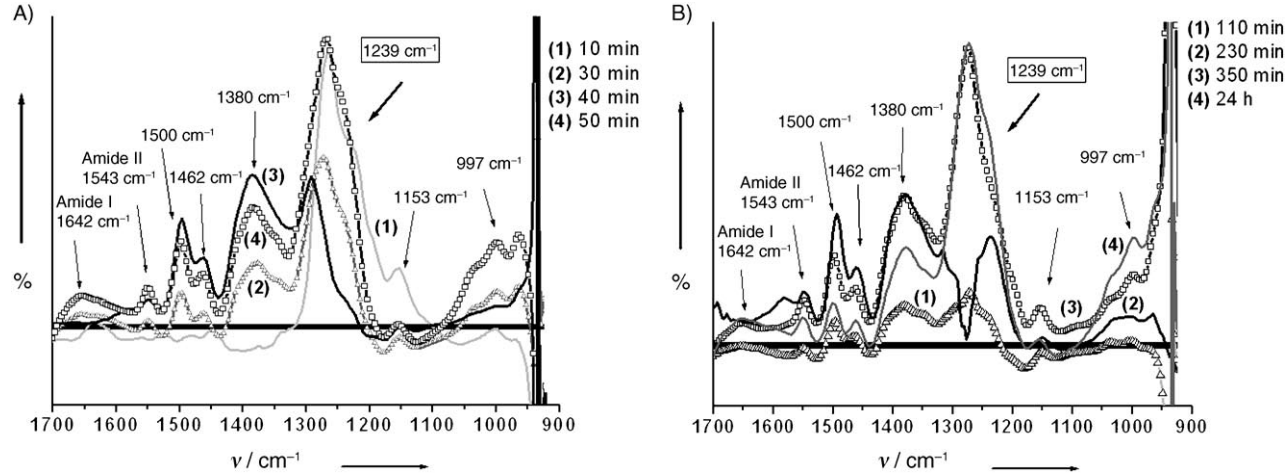

Figure 3. The ratio analysis between the initial stage (t_0) and later stages as t_n/t_0 to determine the relative differences between the two stages. The most clear-cut peaks are indicated and assigned to previously reported bonds (see also Table 1). An alternative version of this figure showing a direct comparison between all time points is given in the Supporting Information.

which were observed less clearly in the original spectra. The ratio of 1 (t_0/t_0) is used as the baseline in order to define either a decreased (ratio < 1) or an increased (ratio > 1) contribution of chemical bonds or interactions at certain frequencies compared to the starting stage of valve formation (t_0). Clearly, the contribution of chemical bonds varied during the course of valve formation in *N. pelliculosa* because the relative contribution of the assigned bonds differed over time (Figure 3). Interestingly, at almost all intervals the relative contribution of amide I and amide II bonds was quite stable in the earliest stages (0–30 min), and clearly was less variable than other bonds with frequencies in the region of 1550 to 1100 cm^{-1} (Figure 3). This suggested that the level of protein synthesis was also quite stable during these earliest stages of valve formation, albeit with the remark that after 30 min the contribution of first amide I ($t > 50$ min) and second amide II ($t > 40$ min) bonds increased. From $t = 30$ min onwards, the contribution of bonds of CH_2NH (1474 cm^{-1}) and of CH_2 and CH_3 groups (both with bands at 1436 cm^{-1}) also increased (Figure 2C). During the course of valve formation, variation in the abundance of P=O bonds (band at 1239 cm^{-1}; Figures 2C and 3) was also observed in the ratio analysis, regardless of the fact that the contribution of these bonds in the normalized spectra (Figure 2C) was quite low. Apparently biomolecules did interact differently at different stages during the course of valve formation in *N. Pelliculosa*.

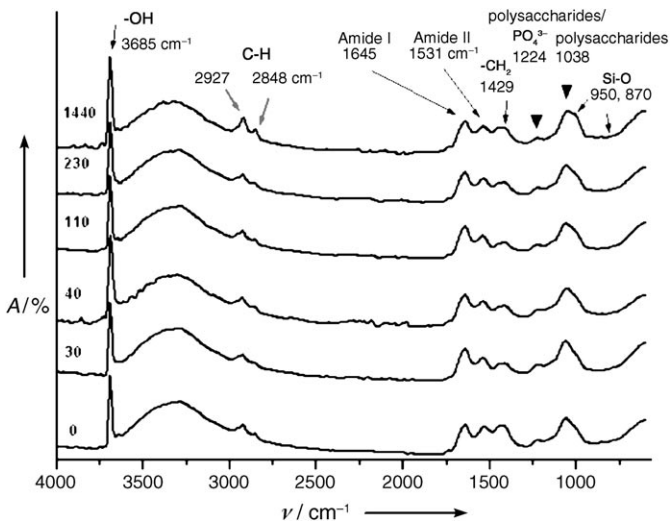

Figure 4. FTIR spectra of the SDS-treated cells of the diatom *Navicula pelliculosa* that were collected during valve formation. The most clear-cut peaks are indicated and assigned to previously reported bonds (see also Table 1). The spectra for the different intervals were vertically shifted for clarity; from bottom to top the following intervals during the course of valve formation in synchronously growing cells are shown: $t = 0$, 30, 40, 110, 230 and 1440 min.

The spectra of the SDS-treated samples of *N. pelliculosa* were much clearer than those that were obtained for the whole cells, and displayed a decreased number of peaks and for several identified bands of lower peak intensities (Figure 4). Certainly the extraction of intracellular matter by SDS has resulted in a diminishment of the contribution of organic matter. The typical band that is observed at 3685 cm^{-1} (arrow Figure 4) was clearly identified in samples of whole cells (Figure 2A), but was much more intense in the spectra of SDS-treated cells. This peak was assigned to O–H stretching that was caused by a hydrated component that interacts with, or is interconnected to a highly ordered or even semi-crystalline structure.[31,38,42,43] In SDS-treated diatom cells, solid silica of the parental frustule and that of newly formed valves contributed mostly (> 90%) to the total sample mass, and exhibited such semicrystalline features (on the micron scale) that relate to homogeneity in pore distributions.[3] Therefore, it was reasonable to suggest that the identified O–H stretching would result from interactions of organic matter, possibly the remnants of the external protective casing or other associated compounds with the solid silica matrix. This suggestion was further supported by the fact that these interactions did not remain when nearly all organic matter was removed by nitric acid oxidation

 © 2008 Wiley-VCH Verlag GmbH & Co. KGaA, Weinheim

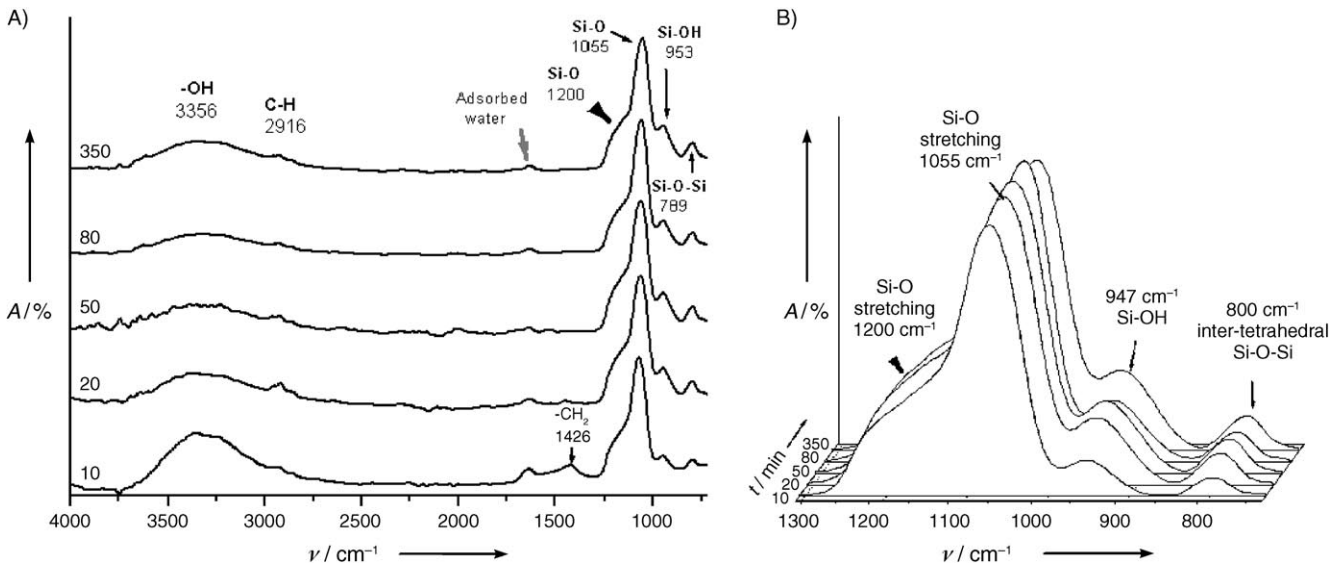

Figure 5. FTIR spectra of the HNO_3-treated cells of the diatom *Navicula pelliculosa* that were collected during valve formation. A) The spectra for the different intervals were vertically shifted for clarity; from bottom to top the following intervals in the course of valve formation in synchronously growing cells are shown: $t = 10$, 20, 50, 80, and 350 min. B) Normalized FTIR spectra for the region 1300–733 cm^{-1} from which the degree of order in the silica network was qualitatively assessed by determining the I_{800}/I_{1055} ratio. For assignment of bands see also Table 1.

(Figure 5). The SDS-treated samples clearly revealed both protein fingerprint bands of amides I and II (Figure 4) and other organic compounds (Table 1). The C–H bonds with typical frequencies at 2927 and 2848 cm^{-1} (gray arrows Figure 4) relate to lipids,[45] whereas the bonds with frequencies at 1224 and 1038 cm^{-1} (arrowheads Figure 4) most probably coincide with phosphorylated compounds and polysaccharides.[31,45] The presence of these compounds indicated that the remnants of the protective casing was still present after SDS treatment, which is in line with previous molecular-probing studies.[46,47]

Most conspicuously, the FTIR spectra of HNO_3-treated samples were nearly void of organic matter, and silica has been retained almost exclusively (Figure 5 A). In fact, HNO_3-treated diatom biosilica, depending on the species, contains at least over 95% silica;[28,42] the organic source most probably consists of analogues of the recently identified silaffins and/or LCPAs, which only can be dissoluted from solid diatom biosilica.[8] Consequently, a low contribution of protein-related bonds in the FTIR spectrum was expected, and only a very small peak was observed at 1632 cm^{-1} (gray arrow Figure 5 A) which is close to the amide II band at 1642 cm^{-1}. Instead of a proteinaceous nature, adsorbed water molecules may also be responsible for this band.[38,48] The main siloxane and silane frequencies are found between 1250 and 950 cm^{-1} (arrows Figure 5 A), while the major Si–O peak was observed at 1055 cm^{-1}, with one additional peak at about 1200 cm^{-1} (arrowheads Figure 5 A and B).

These silica-related bands partially overlap with those that correspond to the presence of carbohydrates and PO_4^{3-} frequencies,[31,34,45,47] which explains why accurate band assignment of silicon-related bonds in the region of 1250–950 cm^{-1} is quite difficult in whole cells (Figure 2) and SDS-treated samples (Figure 4). A wide O–H band with a peak at ~3356 cm^{-1} appeared to decrease in intensity in the course of valve formation in *N. pelliculosa* between the onset (t_0) of valve formation and the nearly 2D completion of the valve after 60 min (see also Figure 1 I and J). The intensity increased again at a later stage (350 min), which can be explained by a second silicification event of, for instance, the synthesis of the girdle bands and/or casing formation before the dividing cells finally separate. Clearly, the previously assigned O–H bands at 3689 and 3685 cm^{-1} that were observed in spectra of whole cells and of SDS-treated cells were absent; this indicates that the observed O–H interactions must occur within the solid silica. Bonds that are related to C–H and C–CH_2 at 2916 and 1426 cm^{-1}, respectively, displayed a low but quite stable intensity over the period of valve formation; this suggests that the contribution of encapsulated organic matter remained constant. By normalizing the spectra for the frequency region between 1300 and 750 cm^{-1} (Figure 5 B), the degree of tetrahedral ordering of SiO_2, or the periodicity of the silica network could be qualitatively assessed by integration of the peak areas and the position of the maxima. By calculation of the ratio I_{800}/I_{1055}, the degree of order was determined, and it was observed that the degree of ordering in the silica network varied in the process of valve formation in *N. pelliculosa* (Table S2in the Supporting Information); the degree of ordering decreased at distinct stages in the following order: $t = 80$, 10, 350, 20 and 50 min. The optimal ordering was seen after 80 min of synchronous growth when the new valves of *N. pelliculosa* became developed completely in their second dimension, as determined by PDMPO probing (Figure 1 J–L). At later stages, the degree of order slightly decreased, which might indicate that completion of the newly formed valves in the third dimension occurs with more hydrated silica on a more dense silica base, namely the completed 2D valve structure.

 © 2008 Wiley-VCH Verlag GmbH & Co. KGaA, Weinheim

Table 1. Assignment of detected FTIR frequencies of inorganic, organic and hybrid bonds for sequentially obtained samples from synchronously growing *Navicula pelliculosa* cells; these samples were examined for intact frozen (column 4) or freeze-dried (column 5) and for cell walls, following treatment of cells with SDS (column 6) or HNO_3 (column 7). The assignment is based on previously reported data (column 3). Frequencies that represent interactions between -OH groups of silica and the C=O esters of a biomolecule are indicated in bold.

Frequency [cm^{-1}]	Assigned bonds	Refs.	Intervals at which bands were identified [min]			
			Whole cells (frozen)	Whole cells (frozen + freeze dried)	SDS-treated cells	HNO_3-treated cells
~3700	Si–OH stretching (disordered)	[19, 22, 23]	n.d.	superimposed on other bands		
~3689 (~3685)	Si–OH stretching (ordered)	[35, 37, 38]	30	50, 350, 1440	0, 30, 40, 110, 230, 1440	n.d.
~3350 (~3338)	O–H stretching	[39, 45]	0, 40, 230	10, 30, 50, 110, 350, 1440	0, 30, 40, 110, 230, 1440	10, 20, 50, 80, 350
~3200	Si–O stretching	[19, 22, 23]		superimposed on other bands		
~2924	C–H stretching	[45]	40, 230	30, 50, 110, 350, 1440	0, 30, 40, 110, 230, 1440	10, 20, 50, 80, 350
2852	C–H stretching	[45]	40, 230	30, 50, 110, 350, 1440	0, 30, 40, 110, 230, 1440	10, 20, 50, 80, 350
1734	C=O	[45]		30, 50, 110, 350, 1440	n.d.	n.d.
1642	amide I	[45]	0, 40, 230	10, 30, 50, 110, 350, 1440	0, 30, 40, 110, 230, 1440	n.d.
1543	amide II	[45]	0, 40, 230	10, 30, 50, 110, 350, 1440	0, 30, 40, 110, 230, 1440	n.d.
1460, 1420	P–O–Si	[35]	–			
~1430	C–CH_2	[45]	0, 40, 230	10, 30, 50, 110, 350, 1440	0, 30, 40, 110, 230, 1440	10, 20
~1563, ~1474	C–NH	[53]	0	10	n.d.	n.d.
~1240	P=O	[31]	230	30, 50, 350, 1440	0, 30, 40, 110, 230, 1440	n.d.
~1165	C–C	[45]	0	50, 1440	–	–
~1140	HPO_4^{2-}	[31]		10	–	–
~1085	Si–O	[22, 23]	0	30, 50, 1440	0, 30, 40, 110, 230, 1440	10, 20, 50, 80, 350
1077	Si–O	[22, 23]		not clear	not clear	10, 20, 50, 80, 350
~1058	P–O–C, Si–O–Si PO_4^{3-}	[19, 22, 23]	0	30, 50, 1440	0, 30, 40, 110, 230, 1440	10, 20, 50, 80, 350
~950, ~870	Si–O	[22, 23]	0, 40, 230	10, 30, 50, 110, 350, 1440	0, 30, 40, 110, 230, 1440	10, 20, 50, 80, 350
~789	Si–O–Si	[22, 23]	n.d.	n.d.	0, 30, 40, 110, 230, 1440	10, 20, 50, 80, 350
Intervals at which PDMPO probed *N. pelliculosa* cells were harvested and their matching samples that were analyzed by FTIR			0, 20, 40, 80, 230, 470	10, 30, 50, 110, 350, 1440	0, 40, 110, 230, 1440	10, 20, 50, 80, 350, 470

n.d.: not detected.

MM+ simulations

To obtain insight into the possible interactions between chemical groups from individual diatomaceous biomolecules or their larger complexes that are due to docking with inorganic groups from silica, we have performed MM+ simulations. By combining geometry optimization and molecular dynamics for establishing relaxation of the optimized structures, we determined a number of local energy minima for every tested biomolecule that was evaluated at different conformations (Table S3). The most stable structure that was obtained for native silaffin-1 corresponded to an α helix conformation with energy of $-3565.67\,kcal\,mol^{-1}$. In this conformation, it was possible for non-ionic silicic acid $Si(OH)_4$ units to approach the regions that are rich in PO_4^{3-} and NH to form hydrogen bonds (Figure 6).

Stretching of the Si–OH bonds, as was noticed in the experimentally obtained FTIR spectra (Figure 5), could even further facilitate such interactions in vivo. In contrast, in the modeled interaction of this molecule with amorphous silica, only weak hydrogen bonds were obtained (Figure 7 A). For the modeled silaffin–silica structure, it was found that oxygen from the phosphate groups from the peptide were responsible for building the hydrogen bonds upon interaction with the amorphous silica structure (Figures 6 and 7). By using the molecular conformation with the lowest energy (Table S3), the distance between the aforementioned groups in the silaffin–amorphous silica models has been determined to be about 2.5 Å in size (Figure 7 A).

 © 2008 Wiley-VCH Verlag GmbH & Co. KGaA, Weinheim

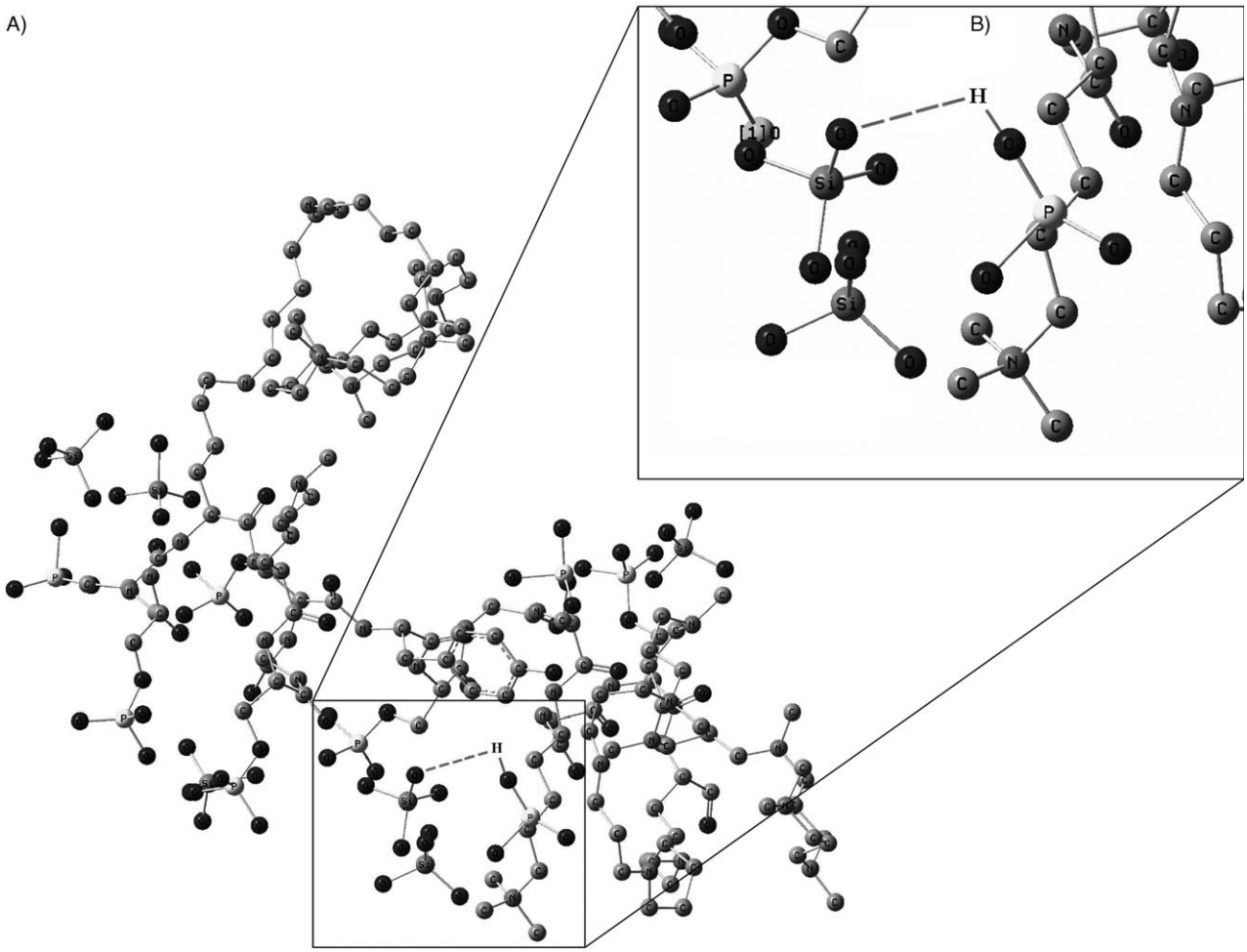

Figure 6. A) The α-helix silaffin model interacting with a $Si(OH)_4$ molecule in a region near a C–H from its side chain (marked box). B) Enlarged view of the $Si(OH)_4$ molecule interacting with the silaffin-1 structure with a PO_4^{3-} group located in the proximity that most probably influences the interaction. The distance between the $Si(OH)_4$ and the molecule is marked with a discontinuous line and has been calculated to be ≈2.5 Å.

FTIR-PM3 simulations

In order to fit the FTIR spectra of our modeled structures to those that were obtained experimentally, we have applied minor horizontal corrections to align the distinctive fingerprint bands, that is, those of the amides (amides I and II) and Si–O, based on their reported assigned frequencies (Table 1). For the organic molecules, a correcting factor of 0.85 was applied, whereas for the silica-related bands the correction factor was 0.90. Despite these minor corrections, we noticed that the simulation of FTIR spectra was not readily straightforward because of the occurrence of a few bands that could not be properly assigned and because of minor variations between multiple simulated FTIR spectra. It is known, however that diversity in FTIR spectra appeared to be caused by small variations in the molecular structures when a molecular dynamic approach is applied. Nevertheless, the simulated FTIR spectra always revealed clear-cut peaks of assignable bonds such as either amide I (at ~1632 cm^{-1}; arrow in Figure 7B) and Si–O (at 741 cm^{-1}; arrowhead in Figure 7B). As stated earlier, the α helix conformation of the modeled native silaffin-1 is the one with the lowest energy, but this conformation might not always occur during silica formation in diatoms, and consequently more bands could be expected. Indeed, our experimental FTIR spectra displayed more assignable bands than the simulated ones (Figures 2–5). Also, in the FTIR simulations, several typical additional bands appeared constantly (asterisks in Figure 7B) that could not be assigned to any chemical bonds so far. These additional bands in the simulated FTIR spectra, however, might have originated from either inharmonic vibrations due to coupling of atoms through the valence electrons in the structures, or heterogeneity in the analyzed system.

Although the simulated FTIR spectra contained minor obscuring signals, the comparison between experimental and simulated FTIR spectra was achieved and provided evidence of variation in silica–biomolecule interactions that specifically occurred during the major silicification event in the synchronously growing diatom *Navicula pelliculosa*, namely the formation of siliceous valves. Such interactions were already suggested by various in vitro studies in which purified diatomaceous biomolecules (e.g., silaffins and LCPAs) or synthetic proteins thereof and other model proteins were used. The assignment of

 © 2008 Wiley-VCH Verlag GmbH & Co. KGaA, Weinheim

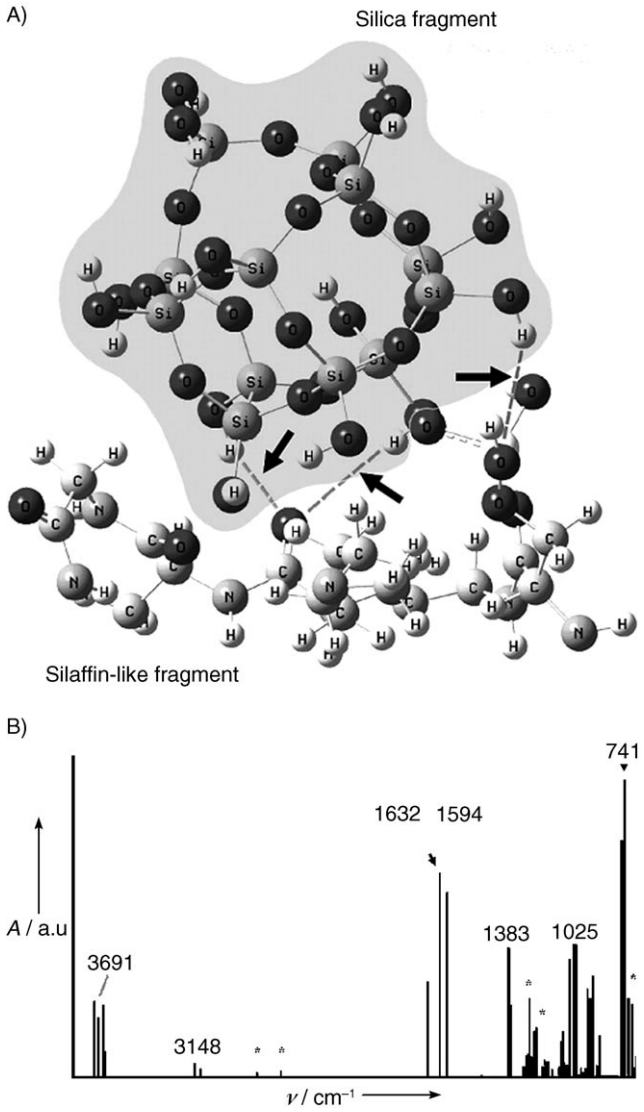

Figure 7. A) Silaffin-1/silica model where the biomolecules in an α-helix conformation interact with the glass-like fragment. The hydrogen bonds are marked as discontinuous lines and black arrows. B) The subsequent simulated FTIR spectrum of the interaction between silica and modeled native silaffin-1 after optimization in water. For details in frequency assignment see Table 1.

bonds that were identified by FTIR also agreed with previously reported data on biosilica,[22,23] but here the dynamics of possible hybrid interactions were analyzed in more detail. FTIR spectra revealed that carboxylic, aliphatic, amine, and possibly also phosphate groups are of main importance in their interactions with silica species in *N. pelliculosa* (Table 1), but the electrostatic interactions could not be excluded. Irrespective of the sample treatment, the typical bands that are related to silica (i.e., those at 1058 and 843 cm^{-1}) were always observed in the FTIR spectra; obviously their contribution increased when organic matter was progressively removed (Figure 2–Figure 5). The identified PO_4^{3-} and carbohydrate bands at 1224 and 1038 cm^{-1}, respectively, in SDS-treated samples (Figure 4) were expected to originate from either the casing components and/or other organic matter that remained firmly associated with, or encapsulated in the diatom biosilica. These bands were absent when cells were treated with nitric acid to remove any bound organic matter (Figure 5). As previously demonstrated, native silaffin appeared to be heavily phosphorylated and modified with polyethyleneimine side chains, and as such, could explain the observed phosphate band. A ^{31}P NMR spectroscopic analysis also demonstrated the presence of phosphate in diatom biosilica.[49] The observed phosphate band was not related to the phosphorus of nucleic acids, because these bonds have different frequencies, namely, at 1100 and 1235 cm^{-1}.[44]

In normalized FTIR spectra for whole cells (Figure 2C), the deformation of weak C–NH or N–H bonds was determined from variations in peaks at 1563 and 1474 cm^{-1}, which were indicative of interactions between both compounds that were facilitated by stretching of hydrogen bonds between the amine groups of a biomolecule towards solid silica. During the course of valve formation in *N. pelliculosa* the contribution of assigned chemical bonds clearly varied (Figure 2–Figure 5), but also suggested that important cellular processes such as protein synthesis (as determined from the presence and contribution of the amide bands in the spectra) were not major events during valve formation. However, upon initiation of valve formation (at $t=0$), immediately following silicon replenishment to cytokinetically arrested *N. pelliculosa* cells, the contribution of most of the assigned bands was much higher. In fact, already after 10 min of silicon replenishment, the relative contribution of all bands had increased in comparison to arrested cells (Figure 2); this implies that the synthesis machineries of both the biomolecules and biosilica were activated substantially. It is also noteworthy that the relative contribution of proteinaceous matter (as defined from the amide bonds) over that of inorganic bonds only increased at stages beyond 40 min of valve formation (Figure 2C). This correlated quite well to our observation of the stage where the siliceous valves of *N. pelliculosa* appeared to be fully developed in their second dimension, (Figure 1I and J) and the dividing cells were preparing for synthesis of the casing[29] and separation.

In the FTIR spectra of whole cells, the presence of the bands that are assigned to N–H stretching (at 3263 cm^{-1}) throughout valve formation was not clear-cut because the relative contribution of such bonds remained stable once silica formation had been initiated (Figure 1A). Only at the earliest stage (<60 min), could organic compounds that display N–H stretching towards silica be involved directly in the rapid silicification process. Indeed our PDMPO probing demonstrated that valve formation is a fast process, and that the 2D completion of the new valve occurs within ~1 hour (Figure 1); this rate of valve synthesis agreed with that of two other species such as the related pennate species *Navicula salinarum*[51] and the centric diatom *Thalassiosira pseudonana*.[52] The band that was observed at 3689 cm^{-1} (Figure 2A, B) appeared at different stages of valve formation, but the presence of these bands always coincided with a C=O band at 1734 cm^{-1} in the FTIR spectra of whole cells (intervals indicated in bold in Table 1). The presence of the C=O band suggests that either an acidic molecule (e.g., with aspartic acid or glutamic acid) has been synthesized

 © 2008 Wiley-VCH Verlag GmbH & Co. KGaA, Weinheim

or that the environmental pH had varied, causing changes in FTIR spectral absorbances of amino acids.[53] For diatoms, it has been demonstrated that the silica deposition vesicle acidifies during valve formation,[46] and that this might explain changes in the spectral behavior of amino acids. The band at 3685 cm^{-1} must be regarded as an assembly of chemical bonds that are related to the silica surfaces at which O–H groups also are present.[37,38,41] In fact, NMR spectroscopic studies on diatom biosilica always proved the presence of Q_1 (SiO–3OH) and Q_2 (SiO_2–2OH) orientations of silica at the surface,[5,41] and it is well possible that these "free" hydroxyl groups form hydrogen bonds with organic molecules such as those that are present in the casing. This assumption was supported by the enhancement of peak intensities of this particular band in FTIR spectra of SDS-treated *N. pelliculosa* cells (Figure 3), where hydrogen bonding of SDS molecules also might have co-occurred.

In general, the biosilica of HNO_3-treated diatoms cells (incl. *N. pelliculosa*) contains $\gg$95% of SiO_2 with a minor amount encapsulated organic matter and trace elements.[5,26] In the samples of *N. pelliculosa* cells that were treated with HNO_3, only a few bands were assigned to organic matter. Based on the assigned P–O–Si bonds with fingerprint bands at 1460 and 1420 cm^{-1} (Figure 6), a covalent linkage between silica and phosphorylated organic molecules or inorganic phosphorus species must have occurred. Remarkably, when covalent P–O–Si bonds were observed, the OH groups with the band located at 3689 cm^{-1} were absent; this makes it tempting to suggest that these hydroxyl groups originated from the silica with hydrogen bridges that interacted with organic compounds. Of interest is whether biomolecules that resemble the native phosphorylated silaffins and LCPAs of *Cylindrotheca fusiformis*, or LCPAs that have been identified in other diatom species also are active in silicification of *N. pelliculosa*.

Conclusions

The experimental data that were obtained indicated that, throughout synthesis of the siliceous valve in cells of the diatom *Navicula pelliculosa*, interactions between inorganic and organic compounds occurred. Theoretically derived data supported the experimental data, and this shows that hybrid interactions between modeled diatomaceous silaffin-1 and silica were favorable when silaffin-1 had an α-helix conformation. As proposed for silaffins and LCPAs on the basis of in vitro studies, silica synthesis and most importantly silica particle size is controlled by the molecular arrangements of chemical groups such as amines and phosphates that are present or interact with the biomolecules.[49,54] Apparently these interactions occurred in vivo too, as has been demonstrated in FTIR spectra on the SDS-treated cell walls of synchronously growing *N. pelliculosa* cells that were collected at various intervals during the course of valve formation. The nature of the interaction most probably relied on hydrogen bonds between the organic compound and silica, but covalent bonds and also electrostatic interactions between silicon and phosphorus could not be excluded. A plausible mechanism for the synthesis of the siliceous frustule parts, is that the local concentration of silicic acid is raised to facilitate rapid polymerization, during which biomolecules in *N. pelliculosa*—possibly analogues of the silaffins or LCPAs currently identified in other species—interact with silica and/or its precursors via hydrogen bonds to further enhance the polymerization process. The presence of bonds between organic and inorganic compounds in HNO_3-treated biosilica samples implied that interacting biomolecules did remain encapsulated in the solid silica structure, as happens to be the case for silaffins and LCPAs. Whether the formation of the characteristic, hierarchically ordered pore structures also relies on similar silica-biomolecules interactions is not clear yet and the controlled synthesis and nanostructural properties of diatom biosilica should be further characterized in this respect to determine the exact role of organic compounds in vivo. For *N. pelliculosa*, the organic structures from which the O–H and C=O bands at respectively 3689 and 1734 cm^{-1} originated, should also be related to the orientation of hydroxyl groups at the surface of the silica that was formed and the distinctive features of the biopolymers that were involved and their properties at different stages of valve development. A detailed understanding of the biomolecule–silica interactions that control biosilica formation is expected to lead to a better understanding of diatom silicon biomineralization, and offers potential for the design of novel synthesis routes for highly ordered silica-based materials.

Experimental Section

Culturing and synchronous growth: An axenic culture (1 L) of the pennate diatom *Navicula pelliculosa* (strain CCMP543) was established in artificial seawater[55] with a salinity of 32.5 practical salinity units (PSU). The cells were grown at 16 °C under a 16 h light/8 h dark cycle by using a light intensity of ~25 μmol photons $m^{-2}s^{-1}$ (Biolux fluorescent tubes, Osram, Germany). The cells were synchronized at the stage of cytokinetic arrest by silica starvation[29] in such a way that immediately after silicon replenishment, valve formation could be evaluated accurately.[51,56] In short, the cells were harvested by mild centrifugation (5 min, 160 *g*, 16 °C) and gently washed twice with silicon-free (Si-free) medium (500 mL). The cells were then resuspended in Si-free artificial seawater (0.5 L) in a 1 L polycarbonate bottle (Nalgene). Cytokinetic arrest was established by 70 h incubation in Si-free medium after synchronous growth was initiated by replenishing the culture with silicic acid (final concentration of 0.20 mM) and the major nutrients nitrate and phosphate (at final concentrations of 340 and 18 μM, respectively).

Sampling and pretreatment of diatom biosilica: Synchronously growing cells were harvested in duplicate at different time intervals for the FTIR spectroscopy experiments (details on the sampling scheme are available in Table 1). For every subsample, the culture (10 mL) was centrifuged (5 min, 890 *g*, 5 °C) and the pelleted cells were subjected to one of the following treatments prior to FTIR analysis: 1) immediately frozen (N_2), 2) immediately frozen (N_2) and subsequently freeze-dried, 3) SDS extraction,[26,51] and 4) HNO_3 extraction.[3,57] Cells that were either solely frozen or frozen and subsequently freeze-dried were examined to determine whether a water effect could be observed in FTIR spectra.

Molecular probing: To evaluate valve morphogenesis in synchronously growing *N. pelliculosa* cells, we applied molecular probing

 © 2008 Wiley-VCH Verlag GmbH & Co. KGaA, Weinheim

by using 2-(4-pyridyl)-5-((4-(2-dimethylaminoethylamino-carbamoyl)methoxy)phenyl)oxazole (PDMPO, LysoSensor yellow/blue DND-160, Molecular Probes, Eugene, USA) as was described previously.[51,58] For this, the probe was simultaneously added at a final concentration of 1.0 μM with silicic acid to the Si-synchronized cells. During valve formation the samples of probed cells (1 mL) were harvested by centrifugation (1 min, 890 *g*, 5 °C) at quite similar intervals to those that were chosen for the FTIR data acquisition (see Table S1). The pelleted cells were immediately resuspended in chilled 98% (*v*/*v*) MeOH (−20 °C; 1 mL) and stored at −20 °C until further microscopic analysis. Fluorescence microscopy was applied by using an Axioscope (Zeiss, Oberkochen, Germany) that was equipped with a bandpass filter for excitation at 365 nm and a longpass filter to record emitted light at wavelengths above 397 nm.

FTIR measurements of diatom biosilica: The FTIR spectra were obtained by using a single-reflectance accessory (Golden Gate, Specac, UK) in an IFS-55 spectrometer (Bruker, Karlsruhe, Germany). The spectra were recorded at the absorbance from 4000 to 600 cm^{-1} at a resolution of 4 cm^{-1} over 128 scans per silica specimen. The penetration depth of the beam was 2 μm[44] and sufficed for a proper analysis of the small diatom species *N. pelliculosa*. To determine the precise frequencies of the different chemical groups that were produced in the experiments, a cross-referencing was performed against previously reported group-specific frequencies (Table 1).

FTIR normalization: To gain insight into the changes in the organic content during valve formation, a normalization by correction for the baseline between the range of 1770–950 cm^{-1} was performed for FTIR spectra that were obtained for whole cells and cell walls that were obtained after HNO_3 extraction. This normalization allowed a qualitative view on changes in bonds over time. In a second step, the normalized spectra were compared to the spectrum at $t=0$ (t_0) by dividing the spectra of later intervals (t_n) by the spectrum of $t=0$. With this approach the difference in intensities of bands became clearer, which made the qualitative analysis more accurate. The chosen region comprised the bands that are known for the amide I, amide II, and biosilica[22,23,45] and could be used as a qualitative index for the content of protein and silica.[23]

To qualitatively determine the different degree of structural ordering of the tetrahedral organization of SiO_2 in the biosilica network over time, a different normalization was implemented in the range of 1300–733 cm^{-1} for the HNO_3-treated samples. Because the HNO_3-treated samples contained only a very limited amount of organic matter, the normalization was based on the integrated surface (*I*) of the silica-related bands that related to the energy that was involved in the FTIR vibration mode, and depended on the mass of silica analyzed.[48] The degree of order in the silica network subsequently was computed according to the half-width and the maximum absorbance (*A*) of the typical bands for silica at 1055 and 800 cm^{-1}. By comparing both *I* and *A* for every interval, it was possible to determine the degree of order in the silica network over time as: $I=\Delta\nu A$, where $\Delta\nu$ is the half-width and *A* the maximum absorbance of the band. The intensity index for every interval was defined as $\Omega=I_{800}/I_{1055}$ and were evaluated for changes during diatom valve formation.[48]

Computational Methods

The MM+ method: Molecular modeling studies were performed by using molecular mechanics and quantum mechanics methods as implemented in the HyperChem program Version 7.1 (HyperCube, Canada). Geometry optimizations were used to find the coordinates of molecular structures that represented a potential energy minimum. Full geometry optimization was performed by using the HyperChem settings for the MM+ force field, the Polak–Ribiere conjugate gradient algorithm, and a root mean square gradient (RMS) of 0.0001 kcal $Å^{-1}$ mol^{-1}. Molecular dynamics relaxation of the optimized structures was employed to look for possible local minima (step size of 0.001 ps, constant simulation temperature of 300 K). The organic molecules were geometrically optimized in both the α-helix and β-sheet to determine the most stable conformation (MM+ method). In the case of the long-chain polyamines (LCPAs) an optimization of the structures with heterogeneous and homogeneous distribution of $[-C_3H_6NCH_3]_n$ was performed. The number of this $[-C_3H_6NCH_3]_n$ group was modified as well, because these chemical modifications affect the functionality and structure of the biomolecules. The models of LCPAs and Silaffin $^1A_1$ (here Silaffin-1) were performed from their most basic structures.[59] Secondary structure models were applied, because data on their three dimensional structures were not available. The organic molecules (see Table S1) were chosen to solely interact with silicic acid in presence of water molecules, and with the non-ionized $Si(OH)_4$ structure; the latter choice was based on the reported non-ionic structure at pH values near 7.0.[60]

The PM3 semi-empirical method: The optimized geometries that were obtained by the MM+ molecular mechanics method were further optimized with PM3 semi-empirical methods by selecting and editing the closest region to the non-ionic $Si(OH)_4$ groups (at least 20 structures were PM3 optimized), by assuming that the closest places are responsible for the formation of the siloxane bonds (Si–O–Si). In semi-empirical calculations, full geometry optimization was performed with the Restricted Hartree–Fock (RHF) basis, Polak–Ribiere conjugate gradient algorithm, and total root-mean-square (RMS) gradient of 0.0001 kcal $Å^{-1}$ mol^{-1} as was recommended in the HyperChem manual, and mentioned previously as the most suitable method for long biomolecules.[61] The HyperChem vibrational spectrum with active IR vector rendering has been used to graphically display the normal modes that were associated with the vibrations. The results of the calculations for the chosen organic molecules are presented in Table S3.

Assignment of simulated IR hybrid bands: The bands of the different hybrid bonds of organic and inorganic groups were simulated in order to approach the silica–biomolecule interaction. The following compounds were optimized with the PM3 method and their bands were obtained: $(OH)_3Si–NH_2$, SiO_2, $H_3C–Si(OH)_3$, $H_3CO–Si(OH)_3$, $(HO)_3P–O–Si(HO)_3$ and non-ionic silicic acid ($Si(OH)_4$) to obtain the Si–N, the Si–O, the Si–C, the Si–O–C, the Si–O–P, and Si–O bands, respectively. In favor of the precise identification of simulated FTIR bands, a minor horizontal correction was performed for matching the well-known SiO_2, amide I, and amide II.

Acknowledgements

A.H. thanks the Deutscher Akademischer Austausch Dienst (Germany) and CONACyT (México) for the financial support to carry out this research. The Technology Foundation STW (grants GFc4983) of the applied science division of NWO and the technology program of the Ministry of Economic Affairs as well as the European Union (SILIBIOTEC grant QLK3-CT-2002–01967) supported the work of E.G.V. and H.S., respectively.

 © 2008 Wiley-VCH Verlag GmbH & Co. KGaA, Weinheim

Keywords: biosilica · chemical bonds · diatoms · IR spectroscopy · molecular modeling · simulations

[1] F. E. Round, R. M. Crawford, D. G. Mann, *Diatoms: Biology and Morphology of the Genera*, Cambridge University, Cambridge, UK, **1990**, p. 757.
[2] E. G. Vrieling, T. P. M. Beelen, R. A. van Santen, W. W. C. Gieskes, *J. Phycol.* **2000**, *36*, 146–159.
[3] E. G. Vrieling, T. P. M. Beelen, Q. Sun, S. Hazelaar, R. A. van Santen, W. W. C. Gieskes, *J. Mater. Chem.* **2004**, *14*, 1970–1975.
[4] R. Gordon, F. Sterrenburg, K. Sandhage, *J. Nanosci. Nanotechnol.* **2005**, *5*, 1–178.
[5] E. G. Vrieling, S. Hazelaar, W. W. C. Gieskes, Q. Sun, T. P. M. Beelen, R. A. van Santen, *Prog. Mol. Subcell. Biol.* **2003**, *5*, 301–334.
[6] R. Gordon, J. Parkinson, *J. Nanosci. Nanotechnol.* **2005**, *5*, 35–40.
[7] Q. Sun, E. G. Vrieling, R. A. van Santen, N. A. J. M. Sommerdijk, *Curr. Opin. Solid State Mater. Sci.* **2004**, *8*, 111–120.
[8] P. J. Lopez, C. Gautiera, J. Livage, T. Coradin, *Curr. Nanosci.* **2005**, *1*, 73–83.
[9] N. Laugel, J. Hemmerle, C. Porcel, J.-C. Voegel, P. Schaaf, V. Ball, *Langmuir* **2007**, *23*, 3706–3711.
[10] M. Sumper, *Science* **2002**, *295*, 2430–2433.
[11] E. G. Vrieling, T. P. M. Beelen, R. A. van Santen, W. W. C. Gieskes, *Angew. Chem.* **2002**, *114*, 1613–1616; *Angew. Chem. Int. Ed.* **2002**, *41*, 1543–1546.
[12] J. D. Pickett-Heaps, D. R. A. Hill, K. L. Blaze, *J. Phycol.* **1991**, *27*, 718–725.
[13] N. Poulsen, N. Kröger, *J. Biol. Chem.* **2004**, *279*, 42993–42999.
[14] C. W. P. Foo, J. Huang, D. L. Kaplan, *Trends Biotechnol.* **2004**, *22*, 577–585.
[15] N. Kröger, R. Deutzmann, C. Bergsdorf, M. Sumper, *Proc. Natl. Acad. Sci. USA* **2000**, *97*, 14 133–14 138.
[16] M. Hildebrand, K. Dahlin, B. E. Volcani, *Mol. Gen. Genet.* **1998**, *260*, 480–486.
[17] K. Shimizu, J. Cha, G. D. Stucky, D. E. Morse, *Proc. Natl. Acad. Sci. USA* **1998**, *95*, 6234–6238.
[18] P. Bhattacharyya, B. E. Volcani, *Proc. Natl. Acad. Sci. USA* **1980**, *77*, 6386–6390.
[19] A. Gelabert, O. Pokrovsky, J. Schott, A. Boudou, A. Feurtet-Mazel, J. Mielczarski, E. Mielczarski, N. Mesmer-Dudons, O. Spall, *Geochim. Cosmochim. Acta* **2004**, *68*, 4039–4058.
[20] M. M. Murr, D. E. Morse, *Proc. Natl. Acad. Sci. USA* **2005**, *102*, 11657–11662.
[21] J. N. Cha, G. D. Stucky, D. E. Morse, T. J. Deming, *Nature* **2000**, *403*, 289–292.
[22] L. G. Benning, V. R. Phoenix, N. Yee, M. J. Tobin, *Geochim. Cosmochim. Acta* **2004**, *68*, 743–757.
[23] L. G. Benning, V. R. Phenix, N. Yee, K. O. Kohnhauser, *Geochim. Cosmochim. Acta* **2004**, *68*, 743–757.
[24] P. D. Tortell, J. R. Reinfelder, F. M. M. Morel, *Nature* **1997**, *390*, 243–244.
[25] E. H. Cox, G. L. McLendon, F. M. M. Morel, T. W. Lane, R. C. Prince, I. J. Pickering, G. N. George, *Biochemistry* **2000**, *39*, 12128–12130.
[26] E. G. Vrieling, T. P. M. Beelen, R. A. van Santen, W. W. C. Gieskes, *J. Biotechnol.* **1999**, *70*, 39–51.
[27] R. K. Iler, *The Chemistry of Silica*, Wiley-Interscience, New York, **1979**, p. 896.
[28] J. D. Pickett-Heaps, A. M. M. Schmid, L. A. Edgar, *Prog. Phycol. Res.* **1990**, *7*, 1–168.
[29] J. Coombs, B. E. Volcani, *Planta* **1968**, *82*, 280–292.
[30] S. A. Crawford, M. J. Higgins, P. Mulvaney, R. Wetherbee, *J. Phycol.* **2001**, *37*, 543–554.
[31] D. Magne, J. Guicheux, P. Weiss, P. Pilet, G. Daculsi, *Calcif. Tissue Int.* **2002**, *71*, 179–185.
[32] http://www.imb-jena.de/ImgLibDoc/ftir/IMAGE_FTIR.html
[33] J. Xu, C. S. Yang, C. K. Choi, *J. Korean Phys. Soc.* **2004**, *45*, 175–179.
[34] Y. H. Shen, S. K. Yao, D. J. Wang, W. Zhou, Y. X. Li, Q. Peng, J. Wu, G.-X. Xu in *9th International Conference On Fourier Transform Spectroscopy, Vol. 2089*, 1st ed., **1994**, SPIE, Calgary, p. 358.
[35] M. D'Apuzzo, A. Aronne, S. Esposito, P. Pernice, *J. Sol-Gel Sci. Technol.* **2000**, *17*, 247–254.
[36] S. H. Kim, E. A. Cherney, R. Hackam, *IEEE Trans. Power Delivery* **1991**, *6*, 1549–1566.
[37] X. B. Yan, B. K. Tay, G. Chen, S. R. Yang, *Electrochem. Commun.* **2006**, *8*, 737–740.
[38] M. W. Urban, *Vibrational Spectroscopy of Molecules and Macromolecules on Surfaces*, Wiley, New York, **1993**, p. 400.
[39] A. N. Lazarev, *Vibrational Spectra and Structure of Silicates*, Consultants Bureau, New York, **1972**, p. 302 (Originally in Nauka Press, USSR **1968**).
[40] R. A. Nyquist, R. O. Kagel, *Infrared Spectra of Inorganic Compounds (3800–45 cm^{-1})*, Academic Press, New York, **1971**, p. 500.
[41] R. Bertermann, N. Kröger, R. Tacke, *Anal. Bioanal. Chem.* **2003**, *375*, 630–634.
[42] R. E. Hecky, K. Mopper, P. Kilham, E. T. Degens, *Mar. Biol.* **1973**, *19*, 323–331.
[43] R. Glenn, S. Sauer, R. E. Wuthier, *J. Biol. Chem.* **1988**, *263*, 13 718–13 724.
[44] J. R. Mourant, Y. R. Yamada, S. Carpenter, I. R. Dominique, J. P. Freyer, *Biophys. J.* **2003**, *85*, 1938–1947.
[45] L. Bellamy, *The Infrared Spectra of Complex Molecules*, 2nd ed., Chapman and Hall, London, **1980**, p. 299.
[46] E. G. Vrieling, W. W. C. Gieskes, T. P. M. Beelen, *J. Phycol.* **1999**, *35*, 548–559.
[47] D. M. Swift, A. P. Wheeler, *J. Phycol.* **1992**, *28*, 202–209.
[48] A. Gendron-Badou, T. Coradin, J. Maquet, F. Frohlich, J. Livage, *J. Non-Cryst. Solids* **2003**, *316*, 331–337.
[49] M. Sumper, E. Brunner, *Adv. Funct. Mater.* **2006**, *16*, 17–26.
[50] M. Cerruti, C. Morterra, P. Ugliengo, *J. Mater. Chem.* **2004**, *14*, 3364–3369.
[51] S. Hazelaar, H. J. van der Strate, W. W. C. Gieskes, E. G. Vrieling, *J. Phycol.* **2005**, *41*, 354–358.
[52] S. Hazelaar, H. J. van der Strate, W. W. C. Gieskes, E. G. Vrieling, M. Hildebrand In: *Nanoscale Architecture; the Role of Proteins in Diatom Silicon Biomineralization* (Ed.: S. Hazelaar), Thesis University of Groningen, Groningen, The Netherlands, **2006**, p. 63–84.
[53] M. Wolpert, P. Hellwig, *Spectrochim. Acta Part A* **2006**, *64*, 987–1001.
[54] K. Lutz, C. Groger, M. Sumper, E. Brunner, *Phys. Chem. Chem. Phys.* **2005**, *7*, 2812–2815.
[55] M. J. W. Veldhuis, W. Admiraal, *Mar. Biol.* **1987**, *95*, 47–54.
[56] W. H. van de Poll, E. G. Vrieling, W. W. C. Gieskes, *J. Phycol.* **1999**, *35*, 1044–1053.
[57] T. Boyle, *Effect of Environmental Contaminants on Aquatic Algae* (Ed.: L. E. Shubert) Academic Press, New York, **1984**, pp. 237–256.
[58] K. Shimizu, Y. Del Amo, M. A. Brzezinski, G. D. Stucky, D. E. Morse, *Chem. Biol.* **2001**, *8*, 1051–1060.
[59] M. Sumper, N. Kröger, *J. Mater. Chem.* **2004**, *14*, 2059–2065.
[60] T. Coradin, P. J. Lopez, *ChemBioChem* **2003**, *4*, 251–259.
[61] V. A. Basiuk, *Spectrochim. Acta A Mol. Biomol. Spectrosc.* **1999**, *55*, 289–298.

Received: June 5, 2007

 © 2008 Wiley-VCH Verlag GmbH & Co. KGaA, Weinheim